An Analytical I-V Characteristics Model for Au-$Al_xGa_{1-x}As$/GaAs VMT Heterojunctions Based on Non-Linear Charge-Control and Field-Dependent Mobility Formulations

H. N. WAZEER
College of engineering – University of Thi-Qar , thiqaruni.org

Abstract

The velocity modulation transistor (VMT) has two channels with differing velocities. Small vertical distance between these channels can be achieved using epitaxial growth, opening the opportunity for higher speed than any other heterostructure field-effect transistor (FET). The non-linear charge-control formulation of the two-dimensional electron gas (2DEG) sheet carriers concentration (n_s), which consider the variation of n_s with Fermi-potential in the triangular potential quantum well of the VMT, has led to a bias-dependent effective offset distance of the 2DEG from the heterointerface. The consideration of variable 2DEG offset distance pushes the model characterization to great accuracy then the linear characterization does. Based on non-linear charge-control and a single set of analytical expressions for field-dependent mobility formulations for $Al_xGa_{1-x}As$/GaAs heterostructure, we developed an analytical I-V characteristics model for VMT device. This model incorporates effects of both composition (x) and doping concentration (N_d) dependences. The model is suitable for computer aided design (CAD) applications in the analysis, design, and optimization of microwave and digital VMT devices.

I. Introduction

The switching time of Field-Effect Transistors (FET's) this is defined as source-drain transit time can be reduced by scaling down the device length [1].

An alternative approach for rapid switching involves transfer carriers between closely spaced layers. Sakaki [2] suggested a device of such real space transfer devices for fast ON-OFF switching that work by velocity modulation, accomplished using two parallel channels having differing mobilities and gave in the name *Velocity Modulation Transistor* (*VMT*). In VMT's drain current is controlled by modulating the carriers velocity in the source-drain channel. As in [2] this concept is shown schematically in Fig.(1). The figure shows structure having a fast top channel, a slow bottom channel, and a two control gates. The electrons are transferred between the two channels due to the application of gate bias. The drain current depends on the gate bias state, which determines the populated channel (high or low-velocity channel). The two gates work in tandem, so when the top gate is high, the bottom gate is low.

The one-dimensional band structure, illustrated for AlGaAs/GaAs heterostructure, is shown in Fig.(2). The velocity difference is achieved by introducing impurities into the low-mobility channel [2]. The high-speed (high-mobility) GaAs channel not contains ionized donors forms the two-dimensional electron gas (2DEG), with donors are located in the neighbouring AlGaAs. The low-speed GaAs channel contains ionized donors. Therefore, velocity modulation is due to different channel mobilities. Fig.(2)a shows the transistor's conduction-band when biased to ON, and the gate nearest the high-mobility channel is positively biased relative to the other gate.

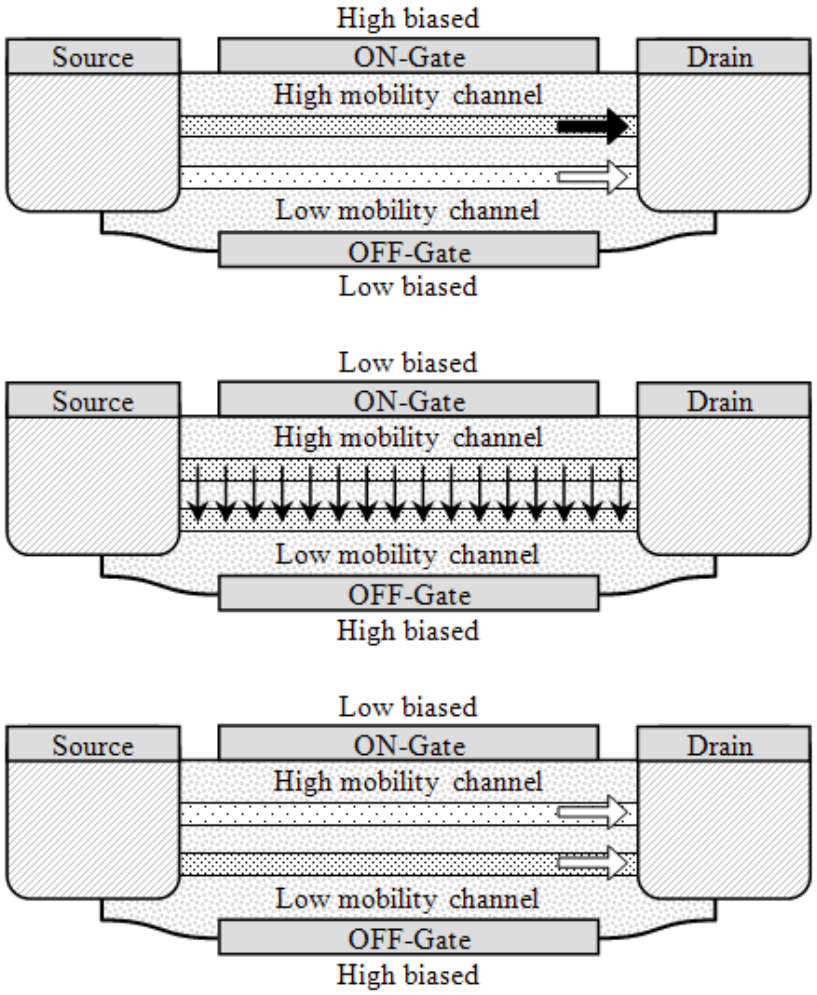

Fig.(1) Schematic of an VMT. Top: the carriers are initially in the top, high-speed channel and the VMT is in the on-state. Middle: the gate voltages are switched and electrons move to the bottom, low-speed channel. Bottom: VMT is in the OFF state.

When the gate biases are reversed, as shown in Fig.(2)b, electrons drift over to the low-mobility channel and the drain current is reduced then the gates are in OFF status. The limiting distance between the two channels is the electron confinement in

the ON and OFF states. Given that the inter-channel transfer time in VMT is less than the transfer time along the channel, the VMT can switches faster than the equivalent heterostructure FET. VMT with small source-drain fields, the velocity difference can be achieved by means of low-mobility differences. At higher fields, differing overshot or saturation drift velocities are necessary. Ideally, one channel has zero velocity, i. e., the operation is one of placing electrons in a reservoir and extracting them back into the channel. However, operation with reservoir would require contacting only one channel (high-speed).VMT drain current-voltage (DC) characteristics are important in predicting its operation or optimizing the performance of its devices and circuits. For accurate prediction and optimization, more accurate and realistic model is needed. Based on analytical non-linear charge-control formulation [3], and a single set of analytical expressions of the field-dependent mobility [4], we develop an analytical VMT I-V characteristics model incorporates

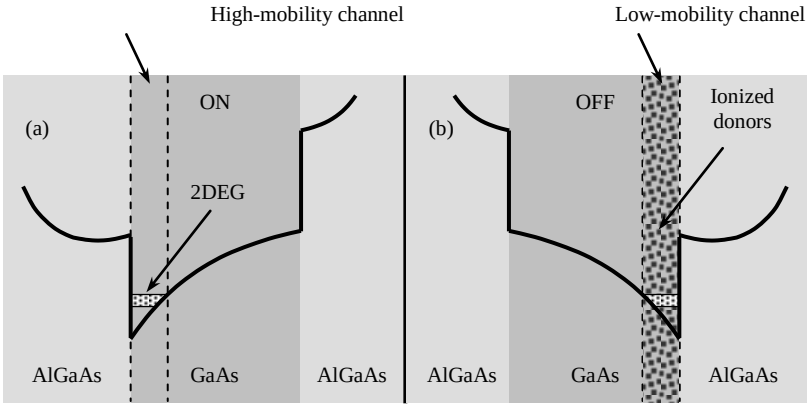

Fig.(2) VMT conduction band: (a) biased to ON, the top gate is positively biased with respect to the other gate and the high-mobility channel is populated; (b) biased to OFF.

both AlGaAs composition (*x*) and GaAs doping level (N_d) for more accuracy.

II. Charge-Control Formulation

The first proposed conventional charge-control model derived from Poisson's equation for heterostructures neglected the Fermi-potential term [5]. The resultant model shows that the channel 2DEG sheet carriers concentration (n_s) depends linearly on the gate bias as

$$n_s(V_G) = \frac{\varepsilon}{qd}(V_G - V_T) \qquad \text{…(1)}$$

***V_T* and *d*, the threshold voltage and the total thickness of the electron supply layer, respectively, are**

$$V_T = \varphi_B - \frac{\Delta E_c}{q} - \frac{qN_d}{2\varepsilon}(d_d)^2 \qquad \text{…(2)}$$

$$d = d_d + d_i \qquad \text{…(3)}$$

where ε is the permittivity of the electron supply layer with a wider energy band gap, q is the electron charge, V_G is the gate-source bias voltage, φ_B is the barrier high of the of the Schottky-gate, ΔE_c is the conduction-band discontinuity at heterojunction, N_d is the doping concentration in the electron supply layer, d_d is the thickness of doped wider band-gap layer, and d_i is the spacer layer thickness.

This model is extended in [6] to include the variation of the 2DEG Fermi-potential with the sheet carrier concentration (n_s). A linear approximation of this variation is

$$V_F = V_{Fo} + a \cdot n_s \qquad \text{…(4)}$$

yields the linear charge-control formulation used by most of the existing analytical I-V characteristics models

$$n_s(V_G) = \frac{\varepsilon}{q(d+\Delta d)}(V_G - V_{Fo} - V_T) \qquad \text{…(5)}$$

where V_{Fo} is the equilibrium Fermi-potential, and Δd is the corresponding offset distance of the 2DEG from the heterointerface. Δd is assumed to have constant value depending on the lattice (a) , i. e.,

$$\Delta d = \frac{\varepsilon \cdot a}{q} \approx 80\,\text{Å} \qquad \text{…(6)}$$

However, the linear charge-control ignores the non-linear dependence of the average position of the 2DEG channel (Δd) from heterointerface on the gate bias. This non-linear dependence is taken into account in [7], where Δd is calculated from the weighted average distance of all energy levels and the total carrier concentration (n_s) in the 2DEG channel calculated as the sum of all occupancy of energy states at various energy levels.

In the triangle potential well approximation, Shey and Ku [3] considered only the lower and the first excited sub-bands. The relation between the sheet carrier concentration (n_s) and the Fermi-level is updated to the simplified, more accurate and non-linear form:

$$E_F = E_{Fo} + \gamma \cdot n_s^{2/3} \qquad \text{…(7)}$$

This non-linear approximation holds as long as the device is not operating in the deep sub-threshold region. Because the potential well broadens remarkably and the sub-bands are closely spaced the quantization effect is of minor importance in this region.

The expression in (7) is valid description of (E_F) versus (n_s) characteristics in all region of interests [3].

Substituting (7) in (1) and rearranging terms, the 2DEG sheet carrier concentration (n_s) can be expressed as:

$$n_s(V,V_G)=\frac{\beta}{(1+\xi(n_s(V,V_G))^{-1/3})}(V_G-V_{To}-V) \qquad \text{…(8)}$$

where V is the source-drain channel potential. The threshold voltage (V_{To}), the linear charge-control coefficient (β), and the offset distance coefficient (ξ) are separately defined as:

$$V_{To}=\varphi_B-\frac{\Delta E_c}{q}+E_{Fo}-\frac{qN_d}{2\varepsilon}(d_d)^2 \qquad \text{…(9)}$$

$$\beta=\frac{\varepsilon}{qd} \qquad \text{…(10)}$$

$$\xi=\frac{\varepsilon\gamma}{qd}=\gamma\beta \qquad \text{…(11)}$$

For AlGaAs/GaAs heterojunction, $\gamma=0.385\times10^{-11}$ eV.m$^{4/3}$ and $E_{Fo}\approx$-0.062 eV [3].

From comparing (5) and (8), it is interesting to note that the corresponding offset distance of the 2DEG (Δd) from the heterojunction is proportional to $n_s^{-1/3}$. This offset distance description will affects the performance significantly [7]. Both, linear and non-linear, charge-control formulations for $Al_xGa_{1-x}As$/GaAs heterostructures did not taken into account the effect of mole fraction (x) on the 2DEG sheet carrier concentration (n_s).

According to [8] and [9], the GaAs dielectric constant (ε), and $Al_xGa_{1-x}As$/GaAs heterostructure band-discontinuity (ΔE_c) are assumed to be functions of mole fraction (x) and can be approximated as:

$$\varepsilon(x)=(13.1-3x)\varepsilon_o \qquad \text{…(12)}$$

$$\Delta E_c(x)=1.06x \ \textbf{(eV)} \qquad \text{…(13)}$$

For Au-AlGaAs junction (the gate metal (Au) and the wide band-gap material junction), the measured Schottky-barrier height (φ_B) can be approximated by [10]:

$$\varphi_B(x)=0.92+0.62x \ \textbf{(eV)} \qquad \text{…(14)}$$

The threshold voltage (V_{To}) as a function of mole fraction (x) and the doping concentration(N_d) of electron supply layer then can be found by substituting (12)-(14) into (9), the substitution yields:

$$V_{To}(N_d,x)=\varphi_B(x)-\Delta E_c(x)-\frac{qN_d}{2\varepsilon(x)}(d_d)^2 \qquad \text{…(15)}$$

Equations (10) and (11) then must be modified to be:

$$\beta(x)=\frac{\varepsilon(x)}{qd} \qquad \text{…(16)}$$

$$\xi(x) = \frac{\varepsilon(x)\gamma}{qd} = \gamma\beta(x) \qquad \text{…(17)}$$

Inserting equations (15)-(17) into (8) yields:

$$n_s(V, V_G, N_d, x) = \frac{\beta(x)\left(V_G - V_{To}(N_d, x) - V\right)}{\left(1 + \xi(x)\left(n_s(V, V_G, N_d, x)\right)^{1/3}\right)} \qquad \text{…(18)}$$

The non-linear charge-control formulation in (18) may be used to study, predict, and optimize the effect of doping concentration (N_d) and the mole fraction (x) for Au-$Al_xGa_{1-x}As$/GaAs heterostructures and devices based on.

III. Field-Dependent Mobility Formulation

Carrier velocity versus longitudinal electric field (*v-E*) characteristic for semiconductor devices contains important information about the field-dependent mobility. This information is useful for the physical modelling of such devices.

In AlGaAs-based devices such as (VMT) [11], an additional complication arises from the effect of composition dependency, which influence electron transport and device performance [12],[13]. As the Aluminium (Al) mole fraction (x) changes, the *v-E* characteristic changes due to the change in the band structure and other transport parameters [4]. There are many different and widely used field-dependent mobility models for GaAs [14]-[16]. However, transport parameters for $Al_xGa_{1-x}As$ are usually extrapolated from those describing GaAs. The electron drift velocity due to parallel electric field (E) is given by:

$$v(E) = \mu(E) \cdot E \qquad \text{…(19)}$$

where $\mu(E)$ is the field-dependent mobility which can be modelled as [14]:

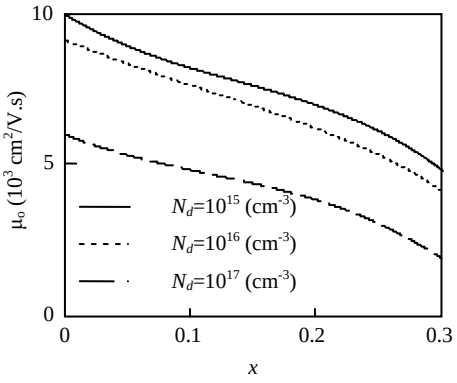

Fig.(3) Low field mobility (μ_o)as a function of $Al_xGa_{1-x}As$/GaAs mole fraction (x) with doping (N_d) as parameter.

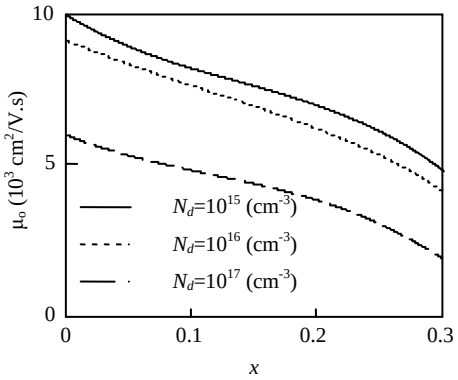

Fig.(3) Low field mobility (μ_o)as a function of $Al_xGa_{1-x}As/GaAs$ mole fraction (x) with doping (N_d) as parameter.

$$\mu(E) = \frac{\mu_o + (v_{sat}/E)(E/E_s)^n}{1+(E/E_s)^n} \qquad \ldots(20)$$

The low-field mobility (μ_o), saturation velocity (v_{sat}), and the critical field for velocity saturation (E_s) are three independent parameters which determine the shape of *v-E* curve. n=4 is found to give the best fit [3].

Based on Monte Carlo formulation technique, Zhou and Tan [4] consider these three parameters to be function of doping concentration (N_d) and composition (x) through equations (21-26). The low-field mobility (μ_o) is expressed as a function of N_d and x by:

$$\mu_o(Nd,x) = \mu_1(x) + \frac{\mu_2(x)}{1+(Nd/N_\mu(x))^{\alpha(x)}} \qquad \textbf{...(21)}$$

where $\mu_1(x)$, $\mu_2(x)$, $N_\mu(x)$, and $\alpha(x)$ are fitting parameters and assumed to be composition dependent. The best polynomials fit these parameters are [4]:

$$\mu_1(x) = \left(0.336 - 0.613x - 0.382x^2\right)\times 10^4 \ \textbf{cm}^2\textbf{/Vs},$$
$$\mu_2(x) = \left(0.6705 - 2.138x + 12.535x^2 - 29.2x^3\right)\times 10^4 \ \textbf{cm}^2\textbf{/Vs},$$
$$N_\mu(x) = \left(6.302 + 7.078x - 59.4x^2\right)\times 10^{16} \ \textbf{cm}^{-3},$$
$$\alpha(x) = 0.957 + 5.908x - 58.3x^2 + 138.2x^3. \qquad \textbf{...(22)}$$

Results of equations (21) and (22) are shown in Fig.(3).

In the same manner, the saturation velocity (v_{sat}) and the critical field for velocity saturation (E_s) are obtained as follows:

$$v_{sat}(N_d,x) = v_o(x) + v_1(x)\left(N_d/N_v(x)\right) + v_2(x)\left(N_d/N_v(x)\right)^{1.04} \ \textbf{...(23)}$$
$$v_o(x) = \left(1.03 + 0.66x - 5.825x^2\right)\times 10^7 \ \textbf{cm/s},$$
$$v_1(x) = \left(-0.1836 - 0.321x\right)\times 10^7 \ \textbf{cm/s},$$
$$v_2(x) = \left(0.1552 + 0.267x\right)\times 10^7 \ \textbf{cm/s},$$

$$N_v(x) = \left(1.714 - 1.6x + 1.825x^2\right) \times 10^{17} \ \textbf{cm}^{-3}. \qquad \textbf{...(24)}$$

$$E_s(N_d, x) = E_o(x) + E_1(x)\left(N_d / N_E(x)\right)^{\rho(x)} \qquad \textbf{...(25)}$$

$$E_o(x) = \left(2.735 + 3.877x - 17.48x^2\right) \ \textbf{kV/cm},$$
$$E_1(x) = \left(0.752 - 0.157x + 15.6x^2 - 65.3x^3\right) \ \textbf{kV/cm},$$
$$N_E(x) = \left(2.14 + 65.045x - 1054.1x^2 + 3486.5x^3\right) \times 10^{16} \ \textbf{cm}^{-3},$$
$$\rho(x) = 0.203 + 1.075x - 15.4x^2 + 48.5x^3. \qquad \textbf{...(26)}$$

The corresponding fitted curves are shown in Fig(4) and Fig(5), respectively.

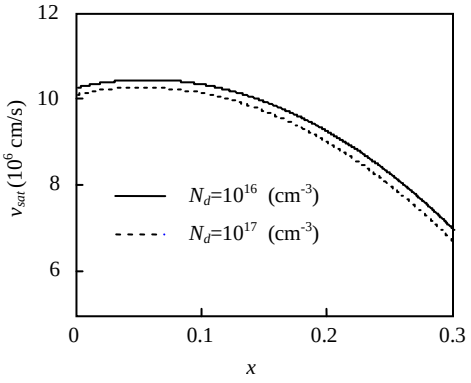

Fig.(4) Saturation velocity (v_{sat}) as a function of $Al_xGa_{1-x}As$/GaAs mole fraction (x) with doping (N_d) as parameter.

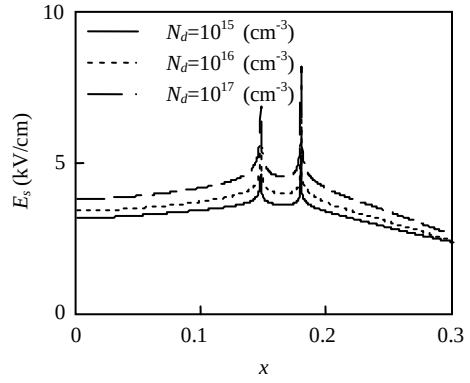

Fig.(5) Critical field for saturation velocity (E_s) as a function of $Al_xGa_{1-x}As$/GaAs mole fraction (x) with doping (N_d) as parameter.

Substituting equations (21), (23), and (25) into (20) yields a new realistic and more accurate field-dependent mobility formulation

$$\mu(E,N_d,x)=\frac{\mu_o(Nd,x)+(v_{sat}(Nd,x)/E)(E/E_s(Nd,x))^n}{1+(E/E_s(Nd,x))^n} \qquad \text{...(27)}$$

This formula for field-dependent mobility is might be suitable for study the behaviour of 2DEG carriers mobility through entering two effective parameters (N_d and x) for $Al_xGa_{1-x}As/GaAs$ heterostructures.

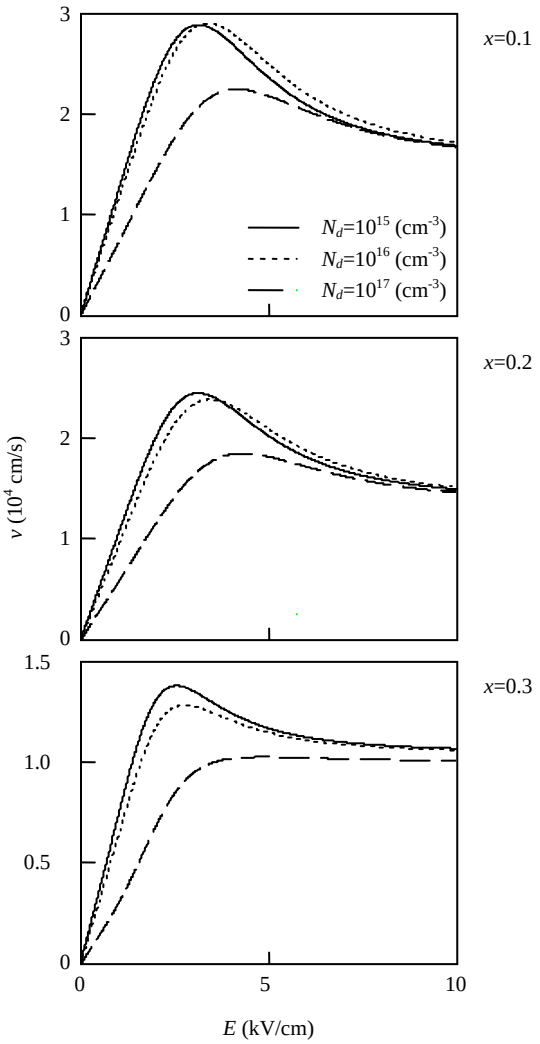

Fig.(6) Carriers velocity (v) versus field (E) characteristics in $Al_xGa_{1-x}As$ with (x) as parameter calculated using equation (27).

The *v-E* curves calculated by using (27) and (19) are shown in Fig.(6). These curves show that the carrier velocity is inversely proportional to both the mole fraction (*x*) and doping concentration (N_d). Values for (*x*) picked to insure a convincing energy band-gap difference between narrow and wide band-gap materials.

IV. I-V Characteristics Model

In the normal (also called intrinsic) operation mode of heterostructure devices (like VMT's) the depletion of the doped layer is from the charge transfer and the Schottky gate depletion. In the normal operation mode, VMT operate in two regions depending on the drain voltage (V_D). These two regions are the linear region ($V_D < V_{Dsat}$) and saturation region ($V_D \geq V_{Dsat}$). Where V_{Dsat} is the drain voltage required by the 2DGE sheet carrier concentration to reach the saturation velocity (v_{sat}). The drain current-voltage (I_D-V_D) curves then can be calculated for each region using the appropriate set of charge-control and velocity-field formulations.

(i) Linear Region ($V_D < V_{Dsat}$):

The region when the applied drain voltage is not high enough to accelerate carriers up to reach the saturation velocity. The linear charge-control formulation in (5) can be used to simplify the non-linear formulation in (18) by ignoring (Δd) and substitute (5) for n_s in the denominator of equation (18). This yields:

$$n_s(V,V_G,N_d,x)=\frac{\beta(x)\left(V_G-V_{To}(N_d,x)-V\right)}{1+\eta(x)(V_G-V_{To}(Nd,x)-V)^{1/3}} \qquad \text{…(28)}$$

where $\eta(x)\,(=\lambda\beta(x)^{2/3})$ **is the non-linear charge-control coefficient.**

In order to obtain an analytical solution, we set *n*=1 in the field-dependent mobility formulation (equation (27)). This assumption yields:

$$\mu(E,N_d,x)=\frac{\mu_o(Nd,x)+(v_{sat}(Nd,x)/E_s(Nd,x))}{1+(E/E_s(Nd,x))}\cdot E \qquad \text{...(29)}$$

The drain current can be evaluated by substituting (28) and (29) into the following equation:

$$I_D = wqn_s v \qquad \text{…(30)}$$

where *w* is the gate width. The substitutions yields

$$I_D(V,V_G,N_d,x)=\frac{w.q.\beta(x)\cdot\left(V_G-V_{To}(Nd,x)-V\right)}{1+\eta(x)(V_G-V_{To}(Nd,x)-V)^{1/3}}\cdot$$

$$\frac{\mu_o(Nd,x)+(v_{sat}(Nd,x)/E_s(Nd,x))}{1+(E/E_s(Nd,x))}\cdot E \qquad \text{...(31)}$$

To simplify the calculations, let *y* defines the inverse offset distance variable as a function of channel potential for the 2DEG channel by:

$$y(V,V_G,N_d,x)=\left(V_G-V_{To}(Nd,x)-V\right)^{1/3} \qquad \text{…(32)}$$

Since the channel potential varies along the channel from source to drain, the boundary condition of the 2DEG channel required that *V* equal to zero at *z*=0 (source terminal) and equal to V_D at $z=L_g$ (drain terminal), where *z* is the direction parallel to the source-drain channel, and L_g is the gate length (here we mean the gate which its bias pushes the VMT ON). Corresponding to this two channel potential values, *y* can be equal to:

$$y_o(V_D,V_G,N_d,x)=\left(V_G-V_{To}(Nd,x)\right)^{1/3} \qquad \text{…(33)}$$

$$y_D(V_D,V_G,N_d,x)=\left(V_G-V_{To}(Nd,x)-V_D\right)^{1/3} \qquad \text{…(34)}$$

Substituting (32) into (31) and integrating *y* from y_o to y_d and *z* from 0 to L_g, we obtain the drain 2DEG current below saturation given by:

$$I_D(V_D,V_G,N_d,x)=\frac{-3A(N_d,x)}{\left(1+\frac{V_D}{\beta(N_d,x)}\right)}\cdot \left[\left[\sum_{n=1}^{6}\frac{(-1)^n}{n}\eta(x)^{(6-n)}\left(\Delta y_D(V_D,V_G,N_d,x)\right)\right]+\eta(x)^6\ln\left(\frac{y_D(V_D,V_G,N_d,x)+\eta(x)}{y_o(V_G,N_d,x)+\eta(x)}\right)\right] \qquad \text{...(35)}$$

where

$$\Delta y_D(V_D,V_G,N_d,x)=\left(y_D(V_D,V_G,N_d,x)\right)^n-\left(y_o(V_D,V_G,N_d,x)\right)^n \qquad \text{…(36)}$$

$$A(N_d,x)=\frac{w\cdot q\cdot\left(\mu_o(N_d,x)+\frac{v_{sat}(N_d,x)}{E_s(N_d,x)}\right)}{L_g} \qquad \text{...(37)}$$

and

$$B(N_d,x)=L_g\cdot E_s(N_d,x) \qquad \text{…(38)}$$

(ii) Saturation Region ($V_D \geq V_{Dsat}$):

When the 2DEG are accelerated to the saturation velocity by the longitudinal electrical field parallel to the current flow, the 2DEG channel current in the saturation region is expressed (by substituting $v=v_{sat}$ and $V=V_{Dsat}$ into (30)) as:

$$I_D(V_D,V_G,N_d,x)=\frac{wq\beta(x)\left(y_s(V_D,V_G,N_d,x)\right)^3 v_{sat}(Nd,x)}{1+\dfrac{\eta(x)}{\left(y_s(V_D,V_G,N_d,x)\right)}} \qquad \textbf{...(39)}$$

where

$$y_s(V_D,V_G,N_d,x)=\left(V_G-V_{To}(N_d,x)-V_{Dsat}\right)^{1/3} \qquad \textbf{...(40)}$$

The velocity of the electron in the channel reaches saturation at the effective channel length ($z=L_s$). Further increase in drain bias will increase the electric field along the channel and cause the electrons to reach saturation velocity at a point closer to the source electrode, i. e., reducing L_s [17]. By requiring the current continuity between the linear and saturation regimes, and by solving the following equation:

$$\lim_{V_D\to V_{Dsat}^-} I_D\big|\ \text{Linear region} = \lim_{V_D\to V_{Dsat}^+} I_D\big|\ \text{Saturtion region} \qquad \textbf{…(41)}$$

we arrive at the expression for the length L_s as a function of x and N_d as:

$$L_s(V_D,V_G,N_d,x)=\frac{-V_{Dsat}}{E_s(Nd,x)}-\frac{3}{E_s(Nd,x)}\cdot\left(\frac{y_s(V_D,V_G,N_d,x)+\eta(x)}{\left(y_s(V_D,V_G,N_d,x)\right)^4}\right)\cdot$$
$$\left[\left[\sum_{n=1}^{6}\frac{(-1)^n}{n}\eta(x)^{(6-n)}\left(\Delta y_s(V_D,V_G,N_d,x)\right)\right]+\right.$$
$$\left.\eta(x)^6\ln\left(\frac{y_s(V_D,V_G,N_d,x)+\eta(x)}{y_o(V_G,N_d,x)+\eta(x)}\right)\right] \qquad \textbf{…(42)}$$

where

$$\Delta y_S(V_D,V_G,N_d,x)=\left(y_S(V_D,V_G,N_d,x)\right)^n-\left(y_o(V_D,V_G,N_d,x)\right)^n \qquad \textbf{…(43)}$$

A relation between L_s and V_{Dsat} is found by [18] as:

$$V_D-V_{Dsat}=\frac{2d_{sat}(N_d,x)E_s(Nd,x)}{\pi}\cdot\sinh\left(\frac{\pi\left(L_g-L_s(V_D,V_G,N_d,x)\right)}{2d_{sat}(V_D,V_G,N_d,x)}\right) \qquad \textbf{…(44)}$$

The effective distance of the saturated 2DEG channel from the gate electrode (d_{sat}) is a function of potential at L_s due to the non-linear charge-control mechanism, namely,

$$d_{sat}(V_D, V_G, N_d, x) = d\left(1 + \eta(x)\left(V_G - V_{To}(N_d, x) - V_{Dsat}\right)^{-1/3}\right) \quad \textbf{…(45)}$$

The value of y_s as a function of V_G and V_D can be found by combining (42)-(45) and using Newton-Raphson's rooting method with initial value set as y_o. Once y_s is known, I_D can be calculated from (39).

The intrinsic I-V characteristic then can be represented by (35) and (39). This model represents the drain current versus drain voltage in one heterostructure in VMT transistor. The current in the second channel (lower mobility channel) can be calculated by using the same derived model after substitute the electronic and physical parameters of the second channel layers. The total drain current is the sum of higher and lower mobility channels currents.

V. Results and discussion

To show the ability of our non-linear model in modelling the I-V characteristics for VMT heterostructures, hereinafter a simulation of these characteristics with respect to N_d and x performed by using MathCAD software. TABLE (I) summarizes the heterostructure VMT parameters used in the simulation for one (higher mobility) heterojunction. Fig. (7) shows the drain current-voltage curves with gate voltage (V_G) as parameter ($I_D(V_D,V_G)$ calculated using (35) and (39). The effect of mole fraction (x) and doping concentration (N_d) on these results, Fig. (8) and Fig. (9) show, respectively, these characteristics. Our model can

TABLE (I)
Device parameters used by the present model

Parameter	Value	Unit
L_g	1	µm
w	145	µm
d_i	20	Å
d_d	80	Å
Δd	80	Å

simulate the $I_D(V_D,V_G)$ curves according to the variation of x, and/or N_d so it is may be used to predict and optimize , with respect to x and N_d, the performance of Au-$Al_xGa_{1-x}As$/GaAs VMT's and their devices. If the gate contact metal changed, the model can be easily modified to fit the new requirements by arranging equation (14) to that control the new metal

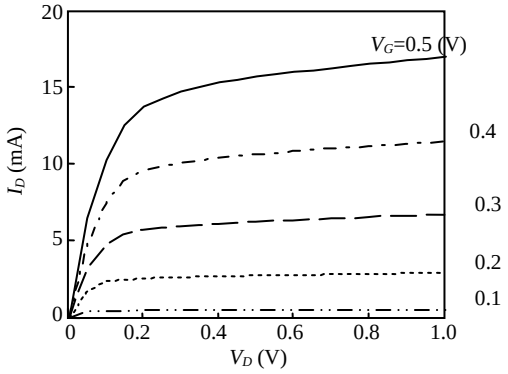

Fig.(7) Drain current-voltage intrinsic characteristics for a VMT fast channel calculated using (35) and (39) with N_d=10^{16} (cm^{-3}) and x=0.3.

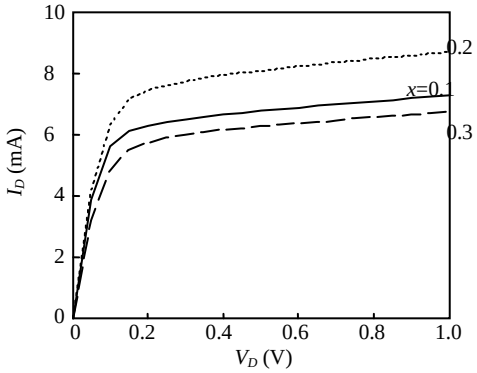

Fig.(8) Drain current-voltage intrinsic characteristics for a VMT fast channel calculated using (35) and (39) with V_G=0.3 (V) and N_d=10^{16} (cm^{-3}).

Schottky-barrier.

This model represent VMT's intrinsic I-V curves, to simulate the extrinsic curves, equations (35) and (39) must be arranged according to the following equations:

$$V_{Dext} = V_D - I_D(R_S + R_D) \qquad \textbf{(46)}$$

$$V_{Gext} = V_G - I_D R_S \qquad \textbf{(47)}$$

where V_{Dext} and V_{Gext} are the extrinsic drain and gate voltages, R_S and R_D are the source and drain resistances.

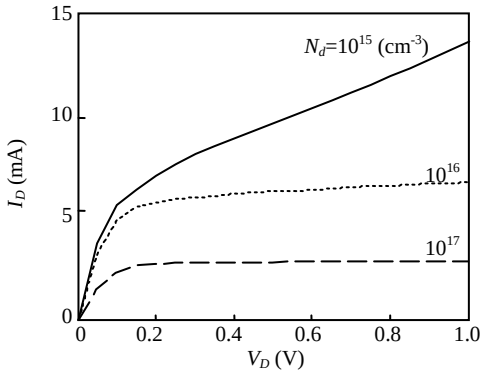

Fig.(9) Drain current-voltage intrinsic characteristics for a VMT fast channel calculated using (35) and (39) with V_G=0.3 (V) and x=0.3.

We have developed an analytical I-V model for heterojunction of VMT that take into account the variation of I-V characteristics curves with both Al-mole fraction and doping concentration based on non-linear charge-control formulation and field-dependent mobility relation. The I-V characteristics can be expressed in an analytical form suitable for the analysis and design of microwave and digital VMT circuits. The model can be applied to optimize and predict the device performance.

References

[1]F. G. Pikus and K. K. Likharev, "Nanosacale field-effect transistor: An ultimate analysis," *Appl. Phys. Lett.* Vol. 71, no. 25, pp. 3661-3663, Dec. 1997.

[2]H. Sakaki, "Velocity-modulation transistor (VMT)- A new field-effect transistor," *Jpn. J. Appl. Phys.*, vol. 21, no. 6, pp.L381-L383, 1982.

[3]An-Jui Shey and Walter H. Ku, "An analytical current-voltage characteristics model for high electron-mobility transistors based on nonlinear charge-control formulation," *IEEE Trans. Electron Devices* vol. 36, no. 10, pp. 2299-2305, 1989.

[4]X. Zhou and H. S. Tan, "Monte carlo formulation of field-dependent mobility for $Al_xGa_{1-x}As$," *Solid-State Electron,* Accepted 22 Sep. 1994.

[5]D. Delagebeaudeuf and N. T. Linh, "Metal-(n) AlGaAs-GaAs two-dimensional electron gas FET," *IEEE Trans. Electron Devices,* vol. ED-29, pp. 955-960, 1982.

[6]T. J. Drummond, H. Morkoc, K. Lee, and M. Shur, "Model for modulation doped field effect transistor," *IEEE Electron Devices Lett.*, vol. EDL-3, pp. 338-341, 1982.

[7]W. A. Hughes and C. M. Snowden, " Nonlinear charge control in AlGaAs/ GaAs modulation doped FET's," *IEEE Trans. Electron Devices,* vol. ED-34, pp. 1617-1625, 1987.

[8]Wen-Chau Liu, Wen-Lung Chan, Wen-Shiung Lour, Kuo-Hui Yu, Chin-Chuan Cheng, and Shiou-Yinh Cheng, "Temperature-dependence investigation of a high performance inverted delta-doped V-shaped GaInP/$In_xGa_{1-x}As$/GaAs pseudomorphic high electron mobility transistor," *IEEE Trans. Electron Devices,* vol. 38, no. 7, pp. 1290-1296, 2001.

[9]M. Keever, K. Hess, and M. Ludowise, "Fast switching and storage in GaAs-$Al_xGa_{1-x}As$ heterojunction layers," *IEEE Electron Devices Lett.*, vol. EDL-3, pp. 297-300, 1982.

[10] Margaret H. Weiler and Yalcin Ayasli, "DC and microwave models for AlGaAs/GaAs high electron mobility transistors," *IEEE Trans. Electron Devices*, vol. ED-31, no. 12, pp. 1854-1816, 1984.

[11] Kevin J. Webb, Erwin B. Cohen, and Michael R. Melloch, "Fabrication and operation of a velocity modulation transistor," *IEEE Trans. Electron Devices*, vol. 48, no. 12, pp. 2701-2709, 2001.

[12] X. Zhou, *IEEE Trans. Electron Devices*, vol. 41, pp. 484, 1994.

[13] I. C. Kizilalli, M. Artaki, and A. Chandra, *IEEE Trans. Electron Devices*, vol. 38, pp. 197, 1991.

[14] J. J. Barnes, R. J. Lomax, and G. I. Haddad, *IEEE Trans. Electron Devices*, vol. ED-23, pp. 1042, 1976.

[15] J. Xu, and M. Shur, *IEEE Trans. Electron Devices*, vol. ED-34, pp. 1831, 1987.

[16] L. F. Eastman, S. Tiwari, M. S. Shur, *Solid –State Electron*, vol. 23, pp. 383, 1980.

[17] D. A. Neamen, "Semiconductor physics and devices, basic principles," *Richard D. Erwin, New York*, pp. 470-479, 1992.

[18] A. B. Grebene and S. K. Ghandhi, "Signal and noise properties of gallium arsenic microwave field-effect transistor," *Solid-State Electron*, vol. 30, pp. 573-589, 1969.